From Oscillation Dip to Oscillation Valley in Atmospheric Neutrino Experiments

Anil Kumar
Research Scholar, India-based Neutrino Observatory (INO)

Collaborators: Amina Khatun, Sanjib Kumar Agarwalla, Amol Dighe

Insitute of Physics, Bhubaneswar

March 11, 2021

Outline

Atmospheric Neutrinos

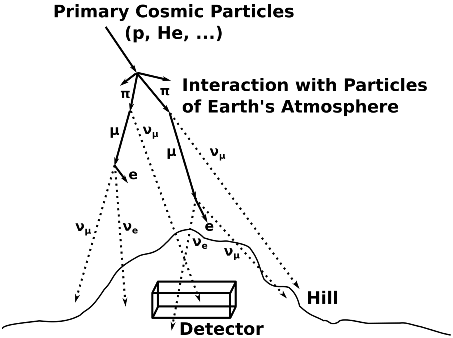

$$\pi^+ \rightarrow \mu^+ + \nu_\mu$$
$$\mu^+ \rightarrow e^+ + \nu_e + \bar{\nu}_\mu$$
$$\pi^- \rightarrow \mu^- + \bar{\nu}_\mu$$
$$\mu^- \rightarrow e^- + \bar{\nu}_e + \nu_\mu$$

Expectation: $\frac{\nu_\mu + \bar{\nu}_\mu}{\nu_e + \bar{\nu}_e} \sim 2$

but at high energies $\frac{\nu_\mu + \bar{\nu}_\mu}{\nu_e + \bar{\nu}_e} > 2$

Baseline and Zenith Angle

- **Upward going Neutrino:**
  $\pi/2 < \theta < \pi$ and $-1 < \cos\theta < 0$
- **Downward going Neutrino:**
  $0 < \theta < \pi/2$ and $0 < \cos\theta < 1$

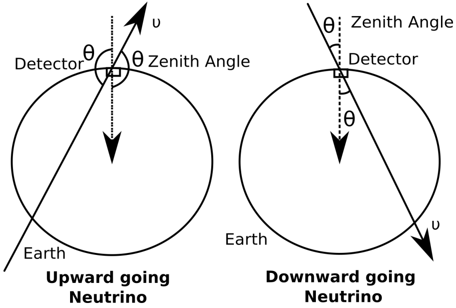

$$L_\nu = \sqrt{(R+h)^2 - (R-d)^2 \sin^2\theta_\nu} - (R-d)\cos\theta_\nu,$$

where R, h, and d denote the radius of Earth, the average height from the surface at which neutrinos are produced, and the depth of the detector underground, respectively. In this study, we take $R = 6371$ km, $h = 15$ km, and $d = 0$ km.

Expected Isotropic Atmospheric Neutrino Flux

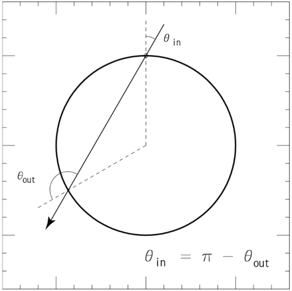

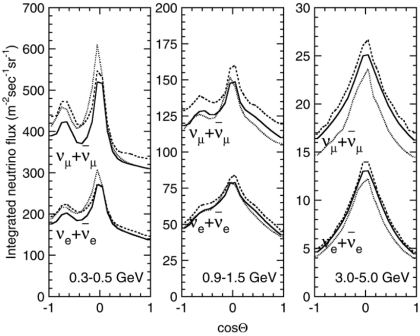

Calculated zenith angle dependence of the atmospheric neutrino flux at Kamioka

- A neutrino trajectory that enters the Earth with zenith angle θ_{in} will exit with a zenith angle $\theta_{\text{out}} = \pi - \theta_{\text{in}}$.
- As far as the primary fuxes are equal at the entry and exit points, one can deduce the up-down symmetry of the neutrino flux.

Takaaki Kajita, 10.2183/pjab.86.303

Observed Asymmetry in Atmospheric Neutrinos Events

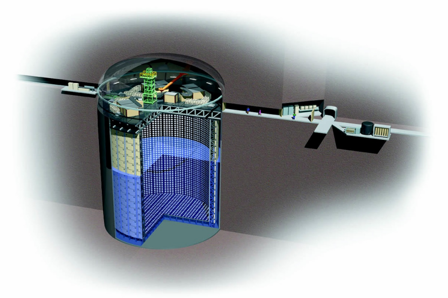

Figure: Super-Kamiokande Detector

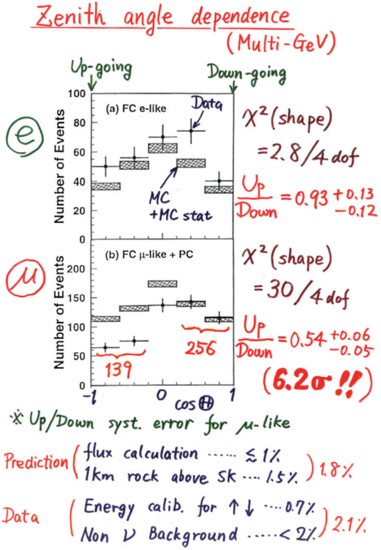

Zenith angle distributions for multi-GeV atmospheric neutrino events presented at the 18th International Conference on Neutrino Physics and Astrophysics (Neutrino'98) by the Super-Kamiokande collaboration (Kajita, 1998)

Takaaki Kajita, 10.1103/RevModPhys.88.030501

Observed Asymmetry in Atmospheric Neutrinos Events

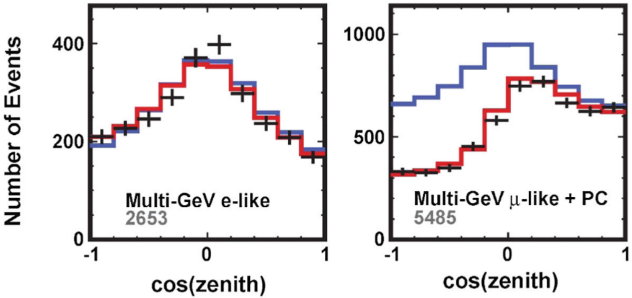

Figure: Zenith angle distribution for multi-GeV e-like (left) and μ-like (right) atmospheric neutrino events observed in Super- Kamiokande (2015).

Takaaki Kajita, 10.1103/RevModPhys.88.030501

Neutrino Oscillations in Two Flavor

The effective Hamiltonion for a neutrino mass eigenstate with mass m_i is

$$H_i = \sqrt{p^2 + m_i^2} \approx p + \frac{m_i^2}{2p} \approx p + \frac{m_i}{2E}$$

For each coherent beam, the time evolution e^{-iHt} contains a common phase e^{-ipt}, which is irrelevant for oscillations. Therefore, $H_i = \frac{m_i^2}{2E}$

$$|\nu_\alpha\rangle = \cos\theta\,|\nu_1\rangle + \sin\theta\,|\nu_2\rangle$$
$$|\nu_\beta\rangle = -\sin\theta\,|\nu_1\rangle + \cos\theta\,|\nu_2\rangle$$

Here, $|\nu_1\rangle$ and $|\nu_2\rangle$ are "mass eigenstates" where as $|\nu_\alpha\rangle$ and $|\nu_\beta\rangle$ are "flavor eigenstates".
After time t,

$$|\nu_\alpha(t)\rangle = \cos\theta\ e^{-\frac{im_1^2 t}{2E}}\,|\nu_1\rangle + \sin\theta\ e^{-\frac{im_2^2 t}{2E}}\,|\nu_2\rangle$$

$$\langle\nu_\alpha|\nu_\alpha(t)\rangle = \cos^2\theta\ e^{-\frac{im_1^2 t}{2E}} + \sin^2\theta\ e^{-\frac{im_2^2 t}{2E}}$$

$$P(\nu_\alpha \to \nu_\alpha) = |\,\langle\nu_\alpha|\nu_\alpha(t)\rangle\,|^2 = 1 - \sin^2 2\theta \sin^2\left(\frac{\Delta m^2 L}{4E}\right)$$

where, $\Delta m^2 = m_2^2 - m_1^2$

Neutrino Oscillations in Three Flavor

$$\nu_\alpha = \sum_i U_{\alpha i} \nu_i$$

$$U = \begin{pmatrix} 1 & 0 & 0 \\ 0 & c_{23} & s_{23} \\ 0 & -s_{23} & c_{23} \end{pmatrix} \begin{pmatrix} c_{13} & 0 & s_{13} e^{-i\delta_{\rm CP}} \\ 0 & 1 & 0 \\ -s_{13} e^{i\delta_{\rm CP}} & 0 & c_{13} \end{pmatrix} \begin{pmatrix} c_{12} & s_{12} & 0 \\ -s_{12} & c_{12} & 0 \\ 0 & 0 & 1 \end{pmatrix}$$

where, $c_{ij} = \cos\theta_{ij}$ and $s_{ij} = \sin\theta_{ij}$.

$$P(\nu_\alpha \to \nu_\beta) = \left| U_{\beta 1} U^*_{\alpha 1} + U_{\beta 2} U^*_{\alpha 2} e^{-i2\alpha\Delta} + U_{\beta 3} U^*_{\alpha 3} e^{-i2\Delta} \right|^2$$

where, $\Delta m^2_{ij} = m^2_i - m^2_j, \quad \alpha = \dfrac{\Delta m^2_{21}}{\Delta m^2_{31}}$ and $\Delta = \dfrac{\Delta m^2_{31} L}{4E}$

In this analysis, we use three-flavor oscillation framework in the presence of matter (PREM profile) with the following values of the benchmark oscillation parameters.

$\sin^2 2\theta_{12}$	$\sin^2 \theta_{23}$	$\sin^2 2\theta_{13}$	$\lvert\Delta m^2_{32}\rvert$ (eV^2)	Δm^2_{21} (eV^2)	$\delta_{\rm CP}$	Mass Ordering
0.855	0.5	0.0875	2.46×10^{-3}	7.4×10^{-5}	0	Normal (NO)

Normal Mass Ordering: $(m^2_3 > m^2_2 > m^2_1)$
Inverted Mass Ordering: $(m^2_2 > m^2_1 > m^2_3)$

Oscillation Dip in Survival Probability

The L/E dependence of survival probability $P(\nu_\mu \to \nu_\mu)$ in two flavor oscillation is given as:

$$P(\nu_\mu \to \nu_\mu) = 1 - \sin^2 2\theta_{23} \cdot \sin^2 \left(1.27 \cdot |\Delta m^2_{32}| \left(\text{eV}^2\right) \cdot \frac{L_\nu\,(\text{km})}{E_\nu\,(\text{GeV})}\right)$$

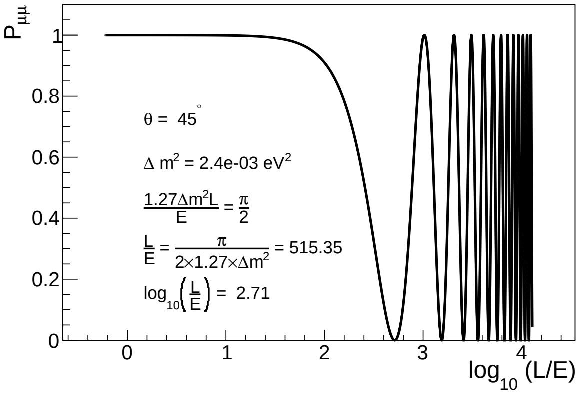

Observation of Oscillation Dip at Super-K Experiment

- The Super-K experiment was the first experiment to observe the sinusoidal L/E dependence of the ν_μ survival probability.
- A dip in the L/E distribution was observed around L/E = 500 km/GeV.
- Neutrino decay and neutrino decoherence models were disfavored in this L/E analysis since they do not predict any dip in the L/E distribution.

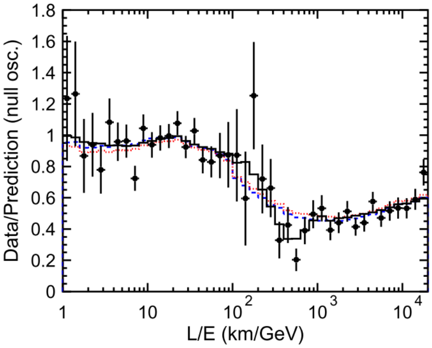

Phys.Rev.Lett. 93 (2004) 101801

Oscillation dip and Oscillation Valley in Survival Channel

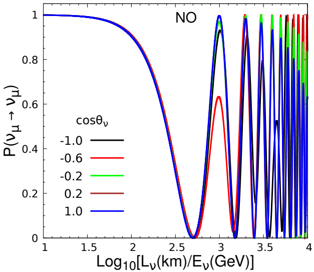

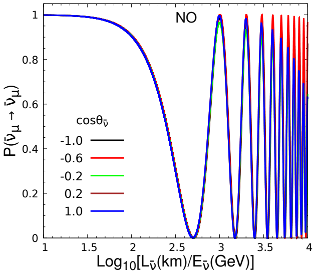

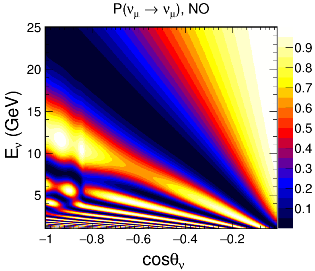

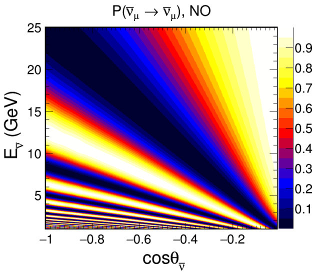

Anil Kumar et. al. EPJC 81, 190 (2021), arXiv:2006.14529

Iron Calorimeter (ICAL) Detector at INO

- **ICAL@INO:** 50 kton magnetized iron detector
- **Active element:** Resistive Plate Chamber (RPC)
- **Passive element:** Iron Plates
- **Uniqueness:** CID for muons, distinguishes ν_μ and $\bar{\nu}_\mu$
- **Muon energy range:** 1 – 25 GeV, **Muon energy resolution:** $\sim 10\%$
- **Baselines:** 15 – 12000 km, **Muon zenith angle resolution:** $\sim 1^\circ$

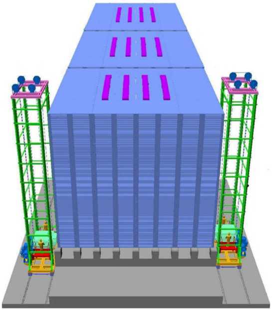

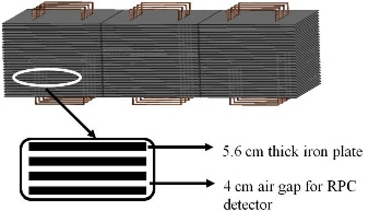

Reconstruction of Oscillation Dip at ICAL

Super-K L/E analysis	Our analysis
Super-K used ratio of data and un-oscillated Monte Carlo to reconstruct dip in L/E distribution.	In our data-driven analysis, we use the ratio of upward-going (U) and downward-going (D) muon events to reconstruct the oscillation dip in $L_\mu^{\rm rec}/E_\mu^{\rm rec}$ distribution.
Super-K analysis used the events with good resolution in L/E. Their analysis rejected neutrino events near the horizon, as well as low-energy events.	The low efficiency of ICAL for near-horizontal event, and our analysis threshold of 1 GeV for muons, automatically incorporates both these filters

U/D ratio (defined for $\cos\theta_\mu^{\rm rec} < 0$)

$$\text{U/D}(E_\mu^{\rm rec}, \cos\theta_\mu^{\rm rec}) \equiv \frac{N(E_\mu^{\rm rec}, -|\cos\theta_\mu^{\rm rec}|)}{N(E_\mu^{\rm rec}, +|\cos\theta_\mu^{\rm rec}|)} ,$$

where $N(E_\mu^{\rm rec}, \cos\theta_\mu^{\rm rec})$ is the number of events with energy $E_\mu^{\rm rec}$ and zenith angle $\theta_\mu^{\rm rec}$.

The U/D ratio automatically cancels most of the systematic uncertainties.

Oscillation Valley Analysis is also Possible at ICAL

Since the ICAL can reconstruct both L_μ^{rec} (hence $\cos\theta_\mu^{rec}$) and E_μ^{rec} accurately, we can go a step ahead and look at the distribution of the U/D ratio in the (E_μ^{rec} , $\cos_\mu^{rec}$) plane to reconstruct "oscillation valley".

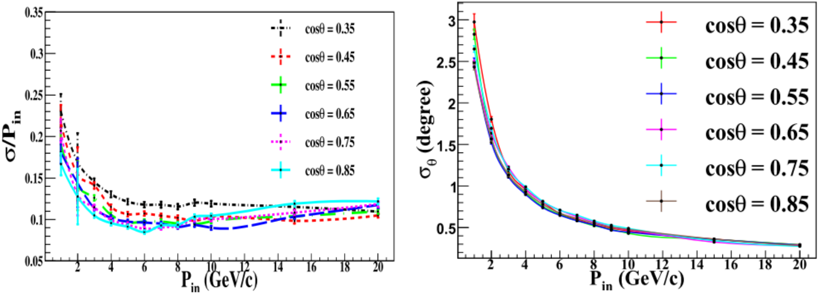

Pramana, Volume 88, Issue 5, article id.79, 72 pp.

Event Generation at ICAL Detector

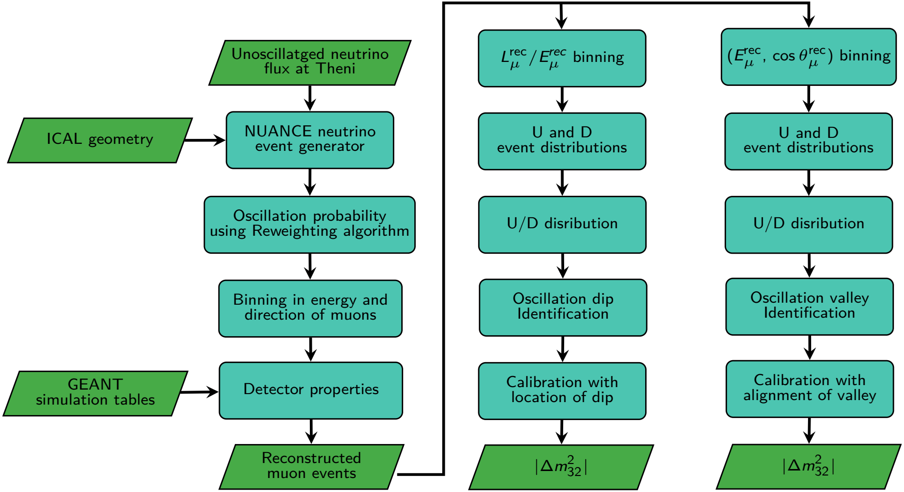

Events and U/D Ratio Using 1000-year MC Simulation

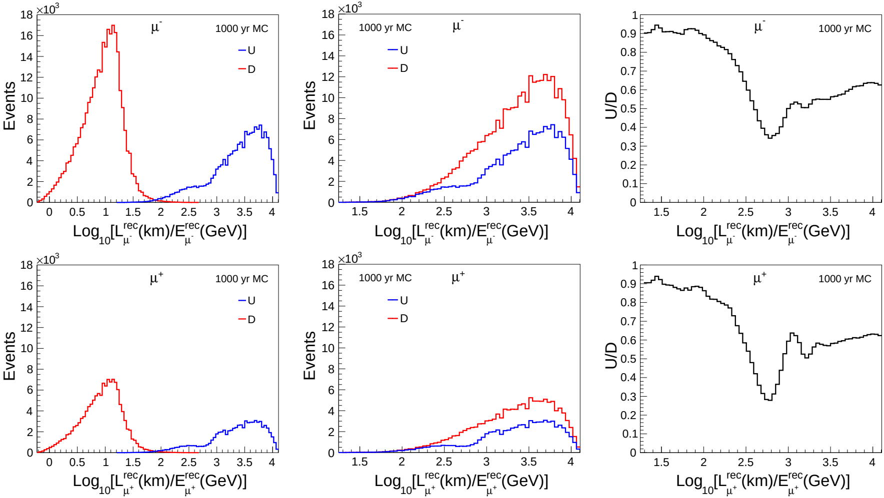

Anil Kumar et. al. EPJC 81, 190 (2021), arXiv:2006.14529

Events and U/D Ratio Using 10-year Simulated Data

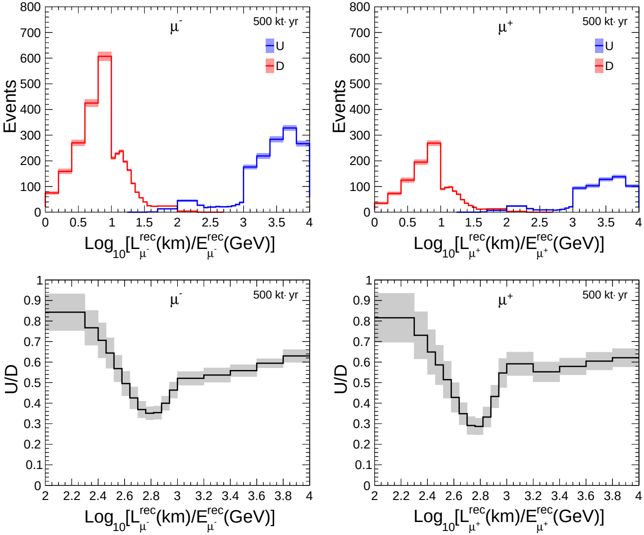

The light colored boxes show statistical uncertainty calculated using 100 simulated sets of 10-year data. (Anil Kumar et. al. EPJC 81, 190 (2021), arXiv:2006.14529)

Dip Identification Algorithm

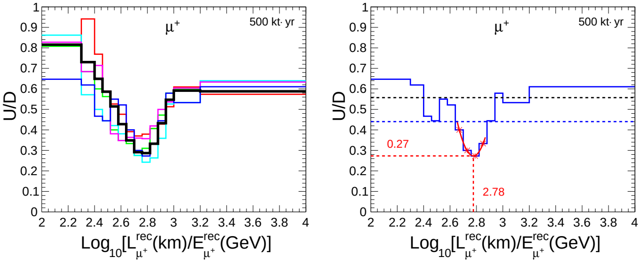

- The left panel shows 5 representative set of 10-year simulated data and thick black line shows mean of 100 simulated sets of 10-year data.
- The right panel shows dip identification algorithm where we start with initial ratio threshold which is shown as dashed black line.
- If ratio threshold passes through more than one oscillation dip then we decrease the ratio threshold.
- The blue dashed line shows the final ratio threshold which passes through only single oscillation dip.
- The bins with U/D ratio less than final ratio threshold are fitted with parabola to obtain location of dip.

Anil Kumar et. al. EPJC 81, 190 (2021), arXiv:2006.14529

Uncertainties in Neutrino Oscillation Parameters

- We first simulated 100 statistically independent unoscillated data sets.
- Then for each of these data sets, we take 20 random choices of oscillation parameters (other than the one going to be measured), according to the gaussian distributions
$\Delta m^2_{21} = (7.4 \pm 0.2) \times 10^{-5}$ eV^2 , $\Delta m^2_{32} = (2.46 \pm 0.03) \times 10^{-5}$ eV^2 , $\sin^2 2\theta_{12} = 0.855 \pm 0.020$, $\sin^2 2\theta_{13} = 0.0875 \pm 0.0026$, $\sin^2 \theta_{23} = 0.50 \pm 0.03$, guided by the present global fit.
- We keep $\delta_{\mathrm{CP}} = 0$, since its effect on ν_μ survival probability is known to be highly suppressed in the multi-GeV energy range.
- This procedure effectively enables us to consider the variation of our results over 2000 different combinations of oscillation parameters, to take into account the effect of their uncertainties.

Anil Kumar et. al. EPJC 81, 190 (2021), arXiv:2006.14529

Systematic Uncertainties

- The five uncertainties are (i) 20% in overall flux normalization, (ii) 10% in cross sections, (iii) 5% in the energy dependence, (iv) 5% in the zenith angle dependence, and (iii) 5% in overall systematics.
- For each of the 2000 simulated data sets, we modify the number of events in each $(E_\mu^{\rm rec}, \cos\theta_\mu^{\rm rec})$ bin as

$$N = N^{(0)}(1+\delta_1)(1+\delta_2)(E_\mu^{\rm rec}/E_0)^{\delta_3}(1+\delta_4\cos\theta_\mu^{\rm rec})(1+\delta_5)\ ,$$

  where $N^{(0)}$ is the theoretically predicted number of events, and $E_0 = 2$ GeV.
- Here $(\delta_1, \delta_2, \delta_3, \delta_4, \delta_5)$ is an ordered set of random numbers, generated separately for each simulated data set, with the gaussian distributions centred around zero and the 1σ widths given by $(20\%, 10\%, 5\%, 5\%, 5\%)$.

Anil Kumar et. al. EPJC 81, 190 (2021), arXiv:2006.14529

Estimating Δm^2_{32} using Location of Dip

- We calibrate Δm^2_{32} with respect to the location of dip using 1000 yr MC.
- The 90% C.L. are obtained using multiple simulated sets of 10-year data.

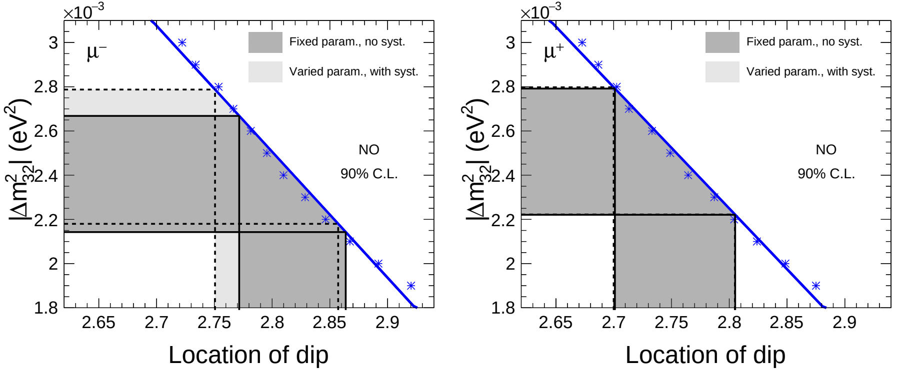

	Δm^2_{32} (in 10^{-3} eV^2) at 90% C.L.			
	μ^-		μ^+	
Fixed param., no syst.	2.14	2.67	2.22	2.79
Varied param., with syst.	2.18	2.79	2.22	2.80

Anil Kumar et. al. EPJC 81, 190 (2021), arXiv:2006.14529

Estimating $\sin^2\theta_{23}$ using the Total U/D Ratio

We use the total U/D ratio of all events with L_μ^{rec}/E_μ^{rec} in the range of 2.2 – 4.1 to give an estimate of $\sin^2\theta_{23}$.

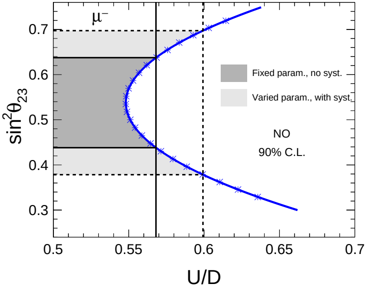

	$\sin^2\theta_{23}$ at 90% C.L.			
	μ^-		μ^+	
Fixed param., no syst.	0.44	0.64	0.39	0.61
Varied param., with syst.	0.38	0.70	0.35	0.65

Anil Kumar et. al. EPJC 81, 190 (2021), arXiv:2006.14529

Events and U/D Ratio Using 1000-year MC Simulation

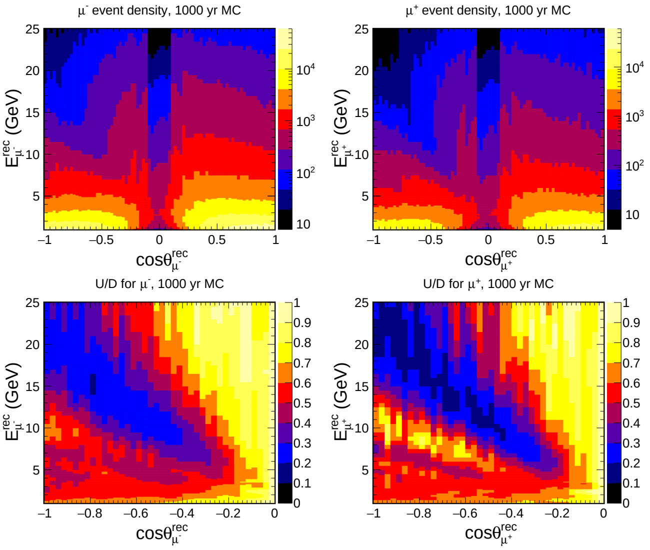

Anil Kumar et. al. EPJC 81, 190 (2021), arXiv:2006.14529

Events and U/D Ratio Using 10-year Simulated Data

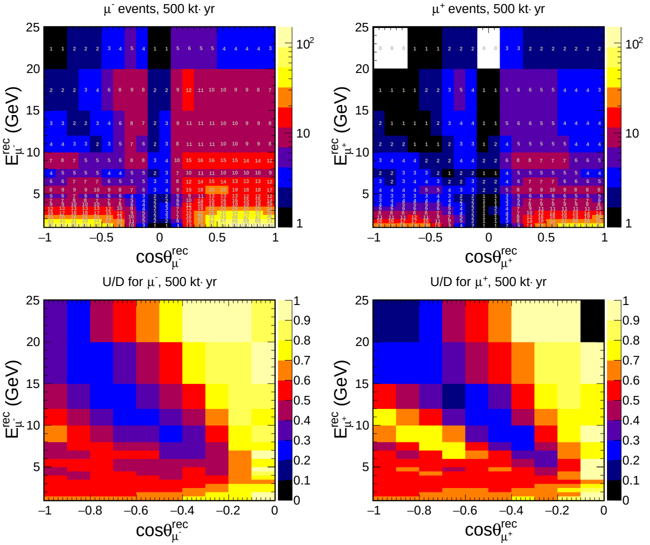

Anil Kumar et. al. EPJC 81, 190 (2021), arXiv:2006.14529

Fitting Oscillation valley

$$F_0(E_\mu^{\rm rec}, \cos\theta_\mu^{\rm rec}) = Z_0 + N_0 \cos^2\left(m_0 \frac{\cos\theta_\mu^{\rm rec}}{E_\mu^{\rm rec}}\right), \quad (1)$$

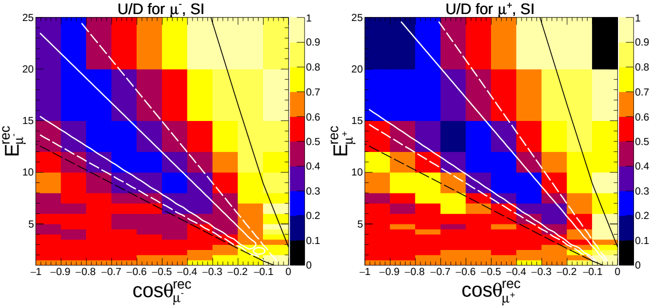

- Mean of 100 U/D distribution for 10 year data.
- Solid black and dashed black lines show conical cut of $\log_{10} L/E = 2.2$ and $\log_{10} L/E = 3.0$ respectively which includes bins used for fitting.
- Solid white and dashed white lines show contours with U/D ratio of 0.4 and 0.5 respectively for fitted function.

Anil Kumar et. al. arXiv: 2101.02607

Estimating Δm^2_{32} using Alignment of Oscillation Valley

- We calibrate Δm^2_{32} with respect to m_0 using 1000 yr MC.
- The 90% C.L. are obtained using multiple simulated sets of 10-year data.

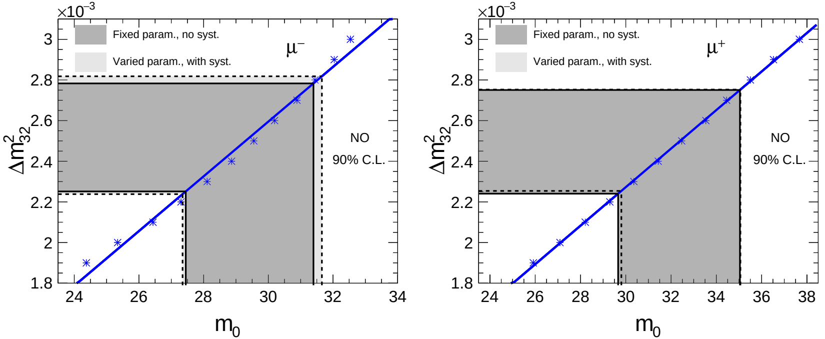

	Δm^2_{32} (in 10^{-3} eV^2) at 90% C.L.			
	μ^-		μ^+	
Fixed param., no syst.	-2.25	-2.78	-2.24	-2.75
Varied param., with syst.	-2.24	-2.82	-2.25	-2.75

Anil Kumar et. al. arXiv: 2101.02607

Summary

- The U/D ratio of muon events was used to reconstuct oscillation dip as a function of $L_\mu^{\text{rec}}/E_\mu^{\text{rec}}$ for μ^- and μ^+ separately..
- We have gone beyond L/E analysis to reconstruct oscillation valley in (E_μ^{rec}, $\cos\theta_\mu^{\text{rec}}$) plane for μ^- and μ^+ separately..
- The location of dip and alignment of valley were used to estimated 90% C.L. for $|\Delta m^2_{32}|$ for μ^- and μ^+ separately.
- The 90% C.L. for θ_{23} was estimated using ratio of total upward-going and total downward-going muon events.

Our procedure can be used for any present or upcoming atmospheric neutrino experiment that has access to a large range of energies and baselines.

Backup: Neutral current Non-Standard Interactions (NSI)

Neutral current NSI in propagation through matter.

$$\mathcal{L}_{\text{NC-NSI}} = -2\sqrt{2}G_F\varepsilon^{Cf}_{\alpha\beta}(\bar{\nu}_\alpha\gamma^\rho P_L \nu_\beta)(\bar{f}\gamma_\rho P_C f)$$

where, $P_L = (1-\gamma_5)/2, P_R = (1+\gamma_5)/2$, and $C = L, R$.

$$\varepsilon_{\alpha\beta} = \sum_{f=e,u,d} \frac{V_f}{V_{CC}} \left(\varepsilon^{Lf}_{\alpha\beta} + \varepsilon^{Rf}_{\alpha\beta}\right)$$

where, $V_{\text{CC}} = \sqrt{2}G_F N_e, V_f = \sqrt{2}G_F N_f, f = e, u, d$.

$$H_{mat} = \sqrt{2}G_F N_e \begin{pmatrix} 1+\varepsilon_{ee} & \varepsilon_{e\mu} & \varepsilon_{e\tau} \\ \varepsilon^*_{e\mu} & \varepsilon_{\mu\mu} & \varepsilon_{\mu\tau} \\ \varepsilon^*_{e\tau} & \varepsilon^*_{\mu\tau} & \varepsilon_{\tau\tau} \end{pmatrix}$$

In atmospheric neutrinos, $\mu - \tau$ channel is dominant, hence, we choose to study about $\varepsilon_{\mu\tau}$

$$H_{mat} = \sqrt{2}G_F N_e \begin{pmatrix} 1 & 0 & 0 \\ 0 & 0 & \varepsilon_{\mu\tau} \\ 0 & \varepsilon^*_{\mu\tau} & 0 \end{pmatrix}$$

Backup: Shift in dip location in reconstructed muon observables

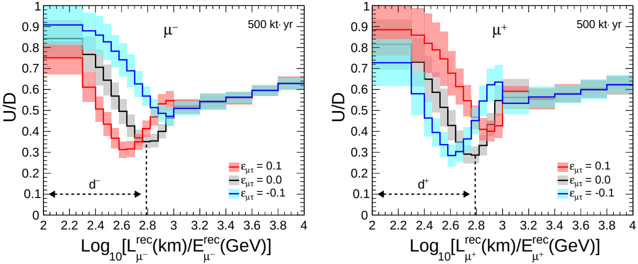

- Statistical uncertainty calculated using 100 simulated sets of 10-year data.
- The location of dip d^- or d^+ depends on magnitude as well as sign of $\varepsilon_{\mu\tau}$.
- d^- and d^+ shift in the opposite direction due to $\varepsilon_{\mu\tau}$.
- d^- and d^+ shift in the same direction due to change in Δm^2_{32}.
- New variable $\Delta d = d^- - d^+$ depends on $\varepsilon_{\mu\tau}$ but independent of Δm^2_{32}(true).

Anil Kumar et al., arXiv: 2101.02607

Backup: Constraints on $\varepsilon_{\mu\tau}$ from measurement of Δd

- We calibrate $\varepsilon_{\mu\tau}$ with respect to Δd using 1000 yr Monte Carlo.
- The 90% C.L. are obtained using multiple simulated sets of 10-year data.

- **Variation over oscillation parameters:** 20 random choices of oscillation parameters for each 10-year simulated data set, according to the Gaussian distribution using σ from current global fit.
- **Systematics errors with Gaussian distributions**: overall flux normalization (20%), cross sections (10%), energy dependence (5%), zenith angle dependence (5%), and overall systematics (5%).

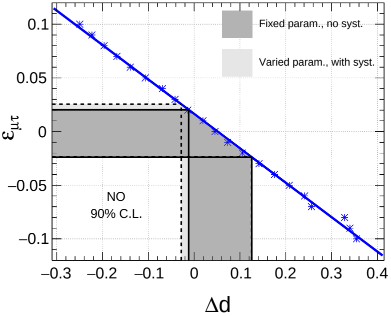

90% C.L.:

- Fixed param., no syst: $-0.024 < \varepsilon_{\mu\tau} < 0.020$
- Varied param., with syst.: $-0.025 < \varepsilon_{\mu\tau} < 0.024$

Anil Kumar et al., arXiv: 2101.02607

Backup: Oscillation valley in neutrino survival probability

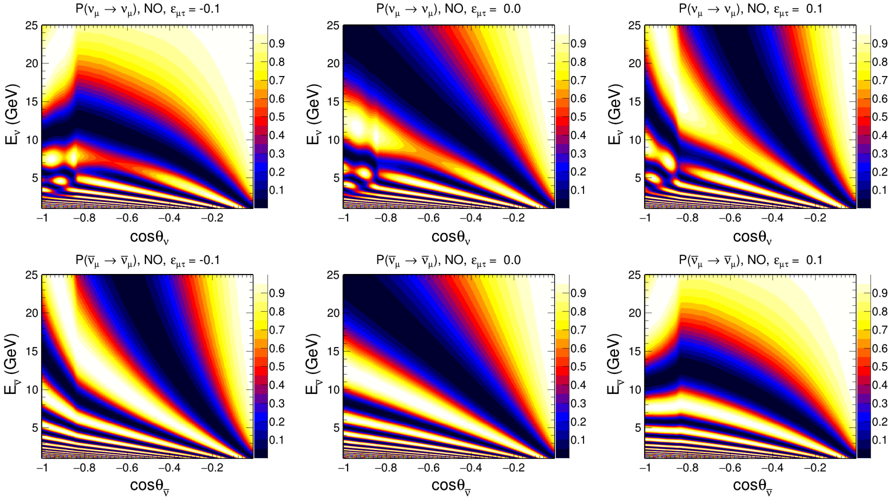

The presence of NSI results in the curvature of oscillation valley (dark blue diagonal band).

Anil Kumar et al., arXiv: 2101.02607

Backup: Identifying NSI through Oscillation Valley

For $\Delta^2_{21} L/4E \rightarrow 0$, $\theta_{13} = 0$, and $\theta_{23} = 45^\circ$, we have[17],

$$P(\nu_\mu \rightarrow \nu_\mu) = cos^2 \left[L \left(\frac{\Delta m^2_{32}}{4E} + \varepsilon_{\mu\tau} V_{CC} \right) \right]$$

Fitting function for oscillation valley

$$f(x, y) = z_0 + N_0 \cos^2 \left(m_\alpha \frac{x}{y} + \alpha x^2 \right)$$

The parameter α is the measure of the curvature of oscillation valley.

[17] Irina Mocioiu et al., Nuclear Physics B 893 (2015) 376–390, arXiv:1410.6193

Backup: Curvature of oscillation valley in reconstructed muon observables

- Mean of 100 U/D distribution for 10 year data in presence of NSI ($\varepsilon_{\mu\tau} = -0.1$ and 0.1).
- Solid black and dashed black lines show conical cut of $\log_{10} L/E = 2.2$ and $\log_{10} L/E = 3.1$ respectively which includes bins used for fitting.
- Solid white and dashed white lines show contours with U/D ratio of 0.4 and 0.5 respectively for fitted function $f(x,y) = z_0 + N_0 \cos^2\left(m_\alpha \frac{x}{y} + \alpha x^2\right)$.

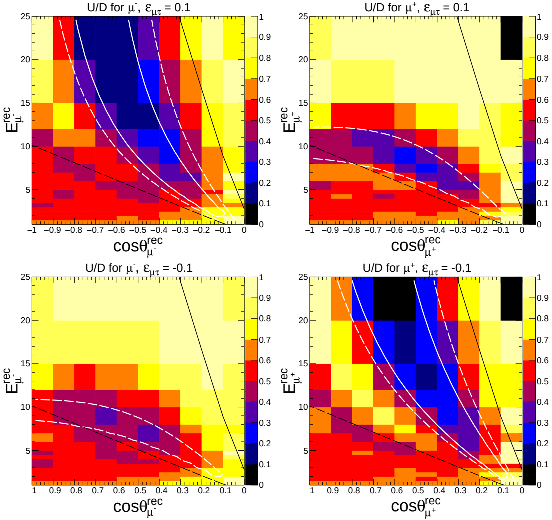

Anil Kumar et al., arXiv: 2101.02607

Backup: Constraints on $\varepsilon_{\mu\tau}$ using curvature of oscillation valley

$\Delta m_\alpha = m_{\alpha^-} - m_{\alpha^+}$ and $\Delta\alpha = \alpha^- - \alpha^+$

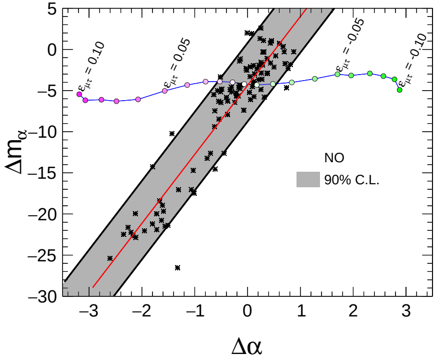

90% C.L.:

- Fixed param., no syst: $-0.022 < \varepsilon_{\mu\tau} < 0.021$
- Varied param., with syst.: $-0.024 < \varepsilon_{\mu\tau} < 0.020$

Anil Kumar et al., arXiv: 2101.02607

Backup: The Binning Scheme for $\log_{10}[L_\mu^{\rm rec}/E_\mu^{\rm rec}]$

Observable	Range	Bin width	Number of bins	
$\log_{10}\left[\frac{L_\mu^{\rm rec}(\text{km})}{E_\mu^{\rm rec}(\text{GeV})}\right]$	[0, 1]	0.2	5	34
	[1, 1.6]	0.06	10	
	[1.6, 1.7]	0.1	1	
	[1.7, 2.3]	0.3	2	
	[2.3, 2.4]	0.1	1	
	[2.4, 3.0]	0.06	10	
	[3, 4]	0.2	5	

Table: The binning scheme adopted for $\log_{10}[L_\mu^{\rm rec}/E_\mu^{\rm rec}]$ for μ^- and μ^+ events of 10-year simulated data.

Backup: The Binning Scheme for Analysis in ($E_\mu^{\rm rec}$, $\cos\theta_\mu^{\rm rec}$) plane

Observable	Range	Bin width	Number of bins	
$E_\mu^{\rm rec}$ (GeV)	[1, 5]	0.5	8	16
	[5, 8]	1	3	
	[8, 12]	2	2	
	[12, 15]	3	1	
	[15, 25]	5	2	
$\cos\theta_\mu^{\rm rec}$	[-1.0, 1.0]	0.1	20	

Table: The binning scheme considered for $E_\mu^{\rm rec}$ and $\cos\theta_\mu^{\rm rec}$ for μ^- and μ^+ events of 10-year simulated data while we show event distribution and U/D plots in the ($E_\mu^{\rm rec}$, $\cos\theta_\mu^{\rm rec}$) plane. This binning scheme is used in analysis of oscillation valley as well.